Supporting Information

Ultra-small Ru nanoparticles embedded on Fe-Ni$(OH)_2$ nanosheets for efficient water splitting at large current density with long-term stability of 680 hours

Huibing Liu[#,1], Qiaohuan Jia[#,1], Shiqing Huang[1], Liu Yang*[,1], Shitao Wang[1], Lirong Zheng*[,2], Dapeng Cao*[,1]

[1] State Key Laboratory of Organic-Inorganic Composites, Beijing University of Chemical Technology, Beijing 100029, People's Republic of China

[2] Beijing Synchrotron Radiation Facility, Institute of High Energy Physics, Chinese Academy of Sciences, Beijing 100049, China

[#] These authors contributed equally to this work.

*Corresponding Authors. E-mail: yl@mail.buct.edu.cn, zhenglr@ihep.ac.cn, caodp@mail.buct.edu.cn

1. Experimental Section

Catalysts Synthesis: The RuFe@NF was synthesized by a simple and mild immersing process. Firstly, the nickel foam (NF) substrate (1 cm × 2 cm) was cleaned sequentially in 3 M HCl, ethanol, and water solution for 15 minutes each through sonication treatment, and then dried at room temperature. Secondly, 97.2 mg of $FeCl_3$ was dissolved in 100 mL of deionized water under vigorous stirring. Afterward, take 5 mL of the above solution into a beaker. To prepare Ru_xFe@NF, different content of Ru (x=0, 0.93 mg, 1.87 mg, 3.37 mg) was added into the above solution, ultrasound 10 min to make it homogeneously dispersed. Finally, the dried NF immersed in the above solution for 6 h. The samples were subsequently removed from the solution, directly dried in air to obtain Ru_xFe@NF samples.

Material Characterizations: The scanning electron microscope (SEM) images of the samples were obtained by HITACHI S-4800. Transmission electron microscopy (TEM) images were performed on a TECNAI G2 F20 field emission transmission electron microscope. The powder X-ray diffraction patterns of the samples were analyzed with an X-ray diffractometer (D8 ADVANCE) using Cu Kα radiation 40 (λ =1.54178 Å). X-ray photoelectron spectroscopy (XPS) measurements were measured on a Thermo Fisher ESCALAB 250 X-ray photoelectron spectrometer equipped with an Al Kα X-ray source. X-ray Absorption Fine Structure (XAFS) was measured at the beam line 4W1B of Beijing Synchrotron Radiation Facility (BSRF), in China. EXAFS data were collected using a fixed-exit double-crystal Si (111) monochromator.

Electrochemical Measurements: All the electrochemical measurements were performed in a general three-electrode system on an electrochemical workstation (CHI760e, Shanghai Chenhua Instrument Factory, China), in which saturated Ag|AgCl regarded as a reference electrode, A carbon rod as the counter electrode and 1 M KOH aqueous solution as electrolyte. For comparison, the commercial catalyst powders (20 wt% Pt/XC-72) was loaded on a pretreated NF with Pt loading of 1 mg on NF (1×1 cm) via drop casting of catalyst ink. The catalyst ink contains 5 mg of catalyst powder, 50 μL of Nafion (117 solution, Aldrich), 800 μL of ethanol, and 200

μL of distilled water.

OER polarization curves obtained from LSV was recorded at a scan rate of 5 mV s^{-1} from -0.2 to 1.0 V *vs*. Ag|AgCl and HER polarization curves was recorded from -0.8 to -1.6 V *vs.* Ag|AgCl. All polarization curves were iR corrected (V'= V-IRs, V' is the corrected potential, V is the original potential, I is current) in this work unless noted otherwise. The overpotential values are defined by the Tafel equation: $\eta=a+b\log|j|$, where η (V) is the overpotential, j (mA cm^{-2}) is the current density, b (mV dec^{-1}) represents the Tafel slope. Electrochemical impedance spectra (EIS) were performed from 100 kHz to 0.1 Hz at 0.47 V *vs.* Ag|AgCl for OER and -1.08 V *vs.* Ag|AgCl for HER. The chronopotentiometry tests were conducted at a constant current density of 10 mA cm^{-2}. CV method was used to measure the electrochemical double layer capacitance (C_{dl}). The potential was swept at different scan rates of 20, 40, 60, 80, and 100 mV s^{-1} from 0.1-0.2 V *vs.* RHE. Electrochemical surface area (ECSA) was calculated by the equation:

$$ECSA = C_{dl}/C_s$$

where C_s is the specific capacitance under specific electrolyte. The value of C_s are intercepted from the literature (Appl. Catal. B: Environ. 2021, 298, 120611).

The TOF of RuFe@NF catalyst was calculated according to the equation (Nat. Commun. 2015, 6, 6616):

$$TOF = \frac{j \times A}{4 \times F \times m}$$

where j is the current density obtained at overpotential of 50 mV, A is the surface area of the integrated electrode (1 cm^2), F is the Faraday efficiency of 96485 C mol^{-1} and m is the number of moles of the Ru on the electrode detected by ICP.

The overall water splitting was carried out in a two-electrode system using RuFe@NF both as the anode and cathode, and the polarization curve was recorded at

a scan rate of 5 mV s^{-1} in 1 M KOH solution with the voltage range from 1.0 V to 2.0 V. For comparison, the commercial Pt/C and IrO_2 as the cathode and anode were also fabricated for the water electrolysis.

2. Supporting Figures

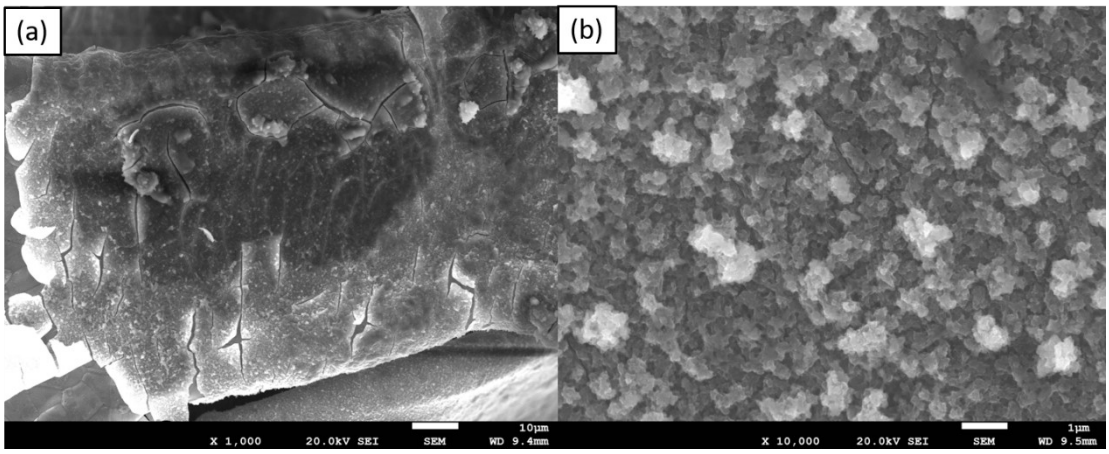

Figure S1. SEM images of RuFe@NF.

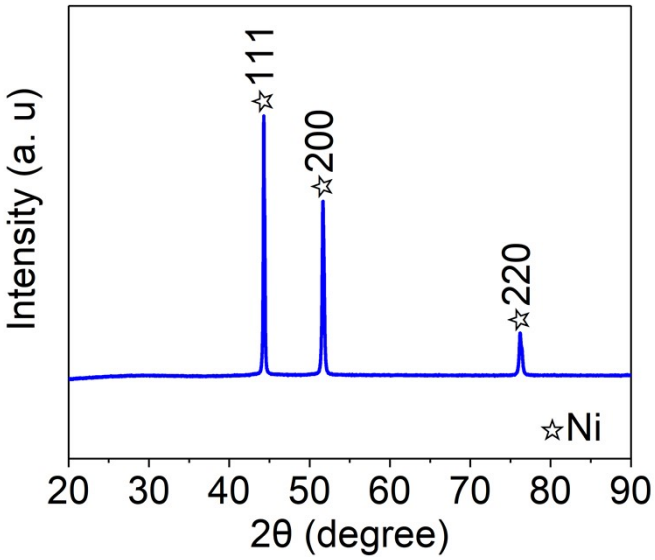

Figure S2. The XRD pattern of RuFe@NF.

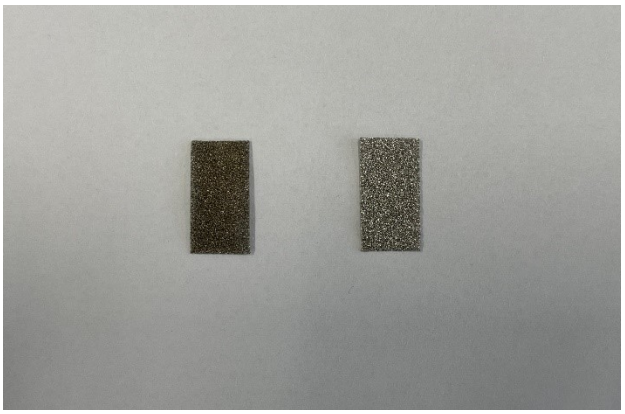

Figure S3. The photograph of RuFe@NF (left) and bare NF (right).

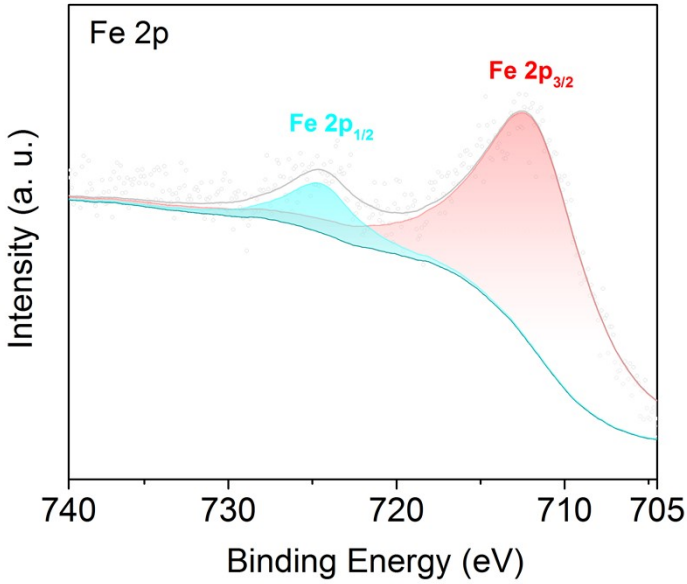

Figure S4. High resolution XPS spectra of Fe2p of RuFe@NF.

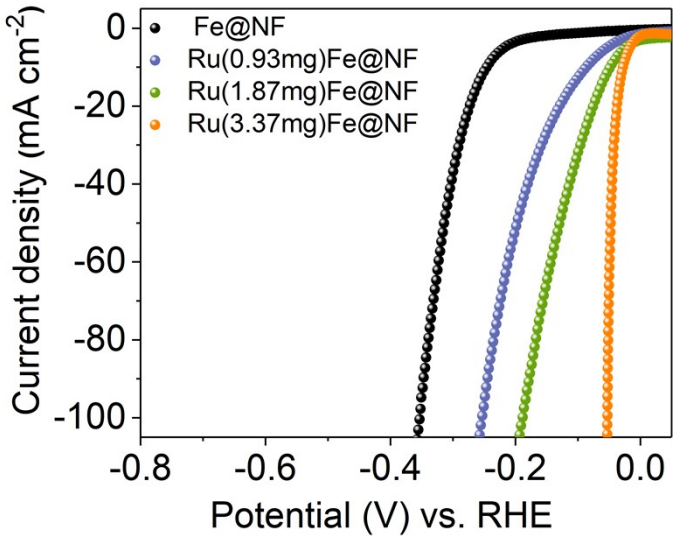

Figure S5. HER polarization curves of Ru_xFe@NF (x=0, 0.93 mg, 1.87 mg, 3.37 mg).

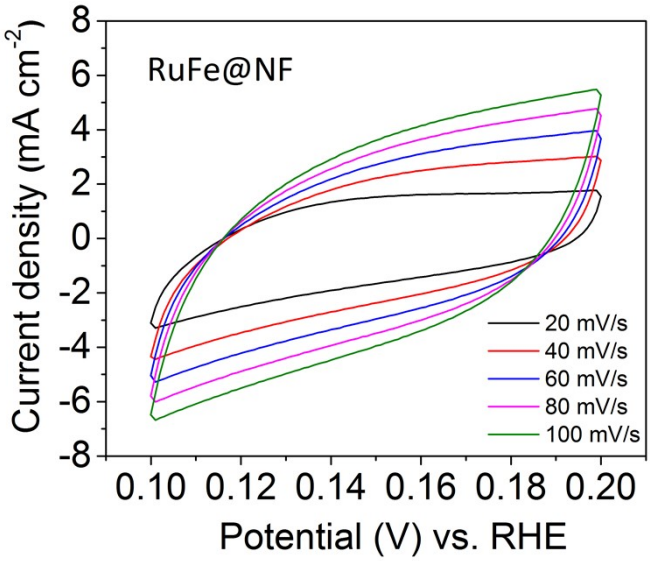

Figure S6. CV curves of RuFe@NF at 0.1-0.2 V *vs.* RHE with the scanning rate ranging from 20 mV/s to100 mV/s.

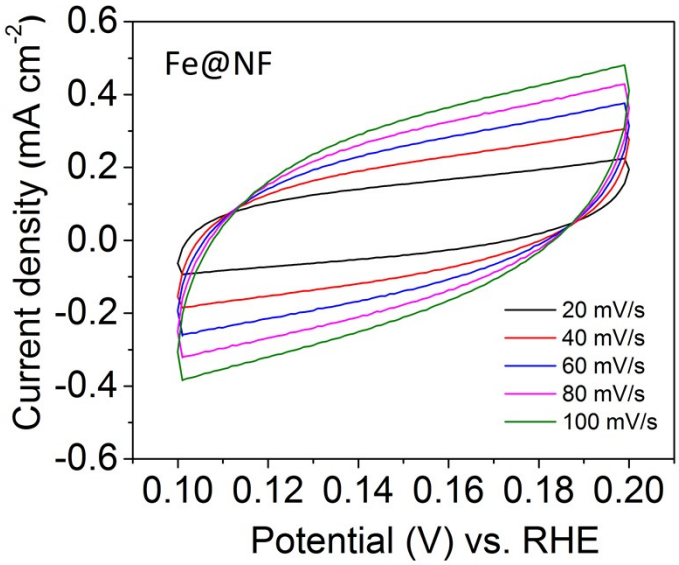

Figure S7. CV curves of Fe@NF at 0.1-0.2 V *vs.* RHE with the scanning rate ranging from 20 mV/s to100 mV/s.

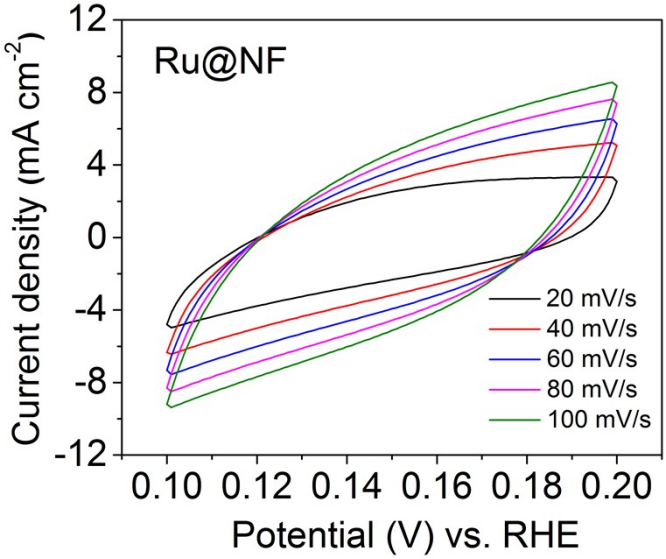

Figure S8. CV curves of Ru@NF at 0.1-0.2 V *vs.* RHE with the scanning rate ranging from 20 mV/s to100 mV/s.

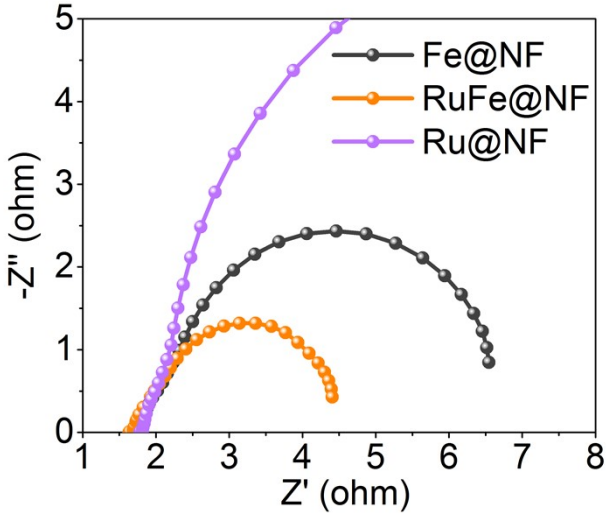

Figure S9. Nyquist plots of RuFe@NF, Fe@NF and Ru@NF for OER.

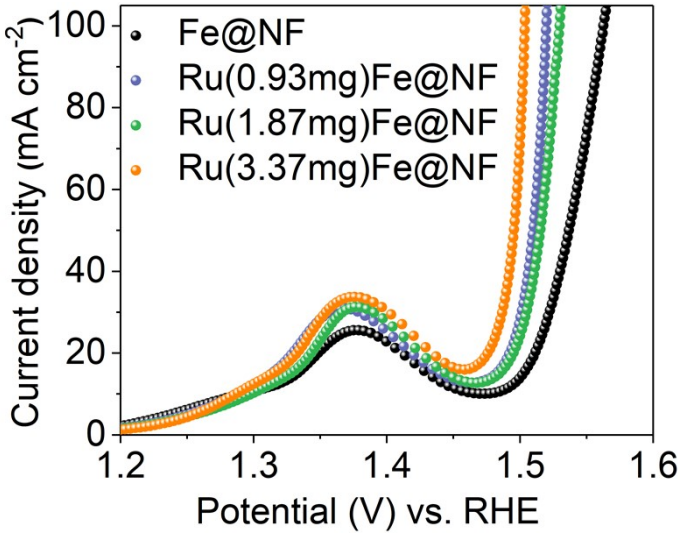

Figure S10. OER LSV curves of Ru_xFe@NF (x=0, 0.93 mg, 1.87 mg, 3.37 mg).

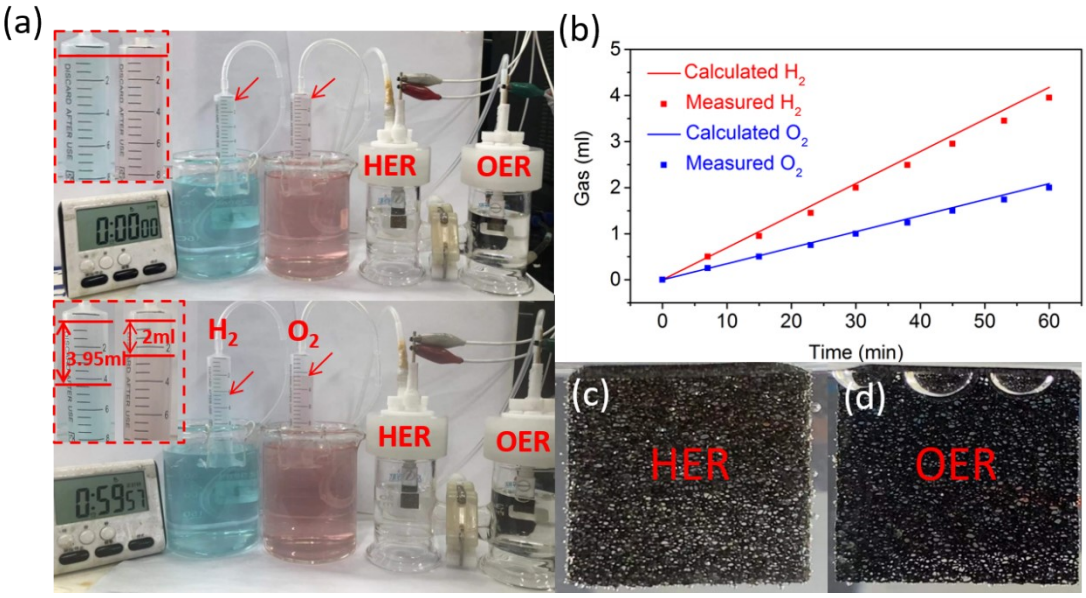

Figure S11 (a) Digital image of the collected gas from water-splitting device. (b) Measured and calculated H_2 and O_2 in cathode and anode, respectively. The digital images of bubbles on the (c) cathode and (d) anode electrode surface.

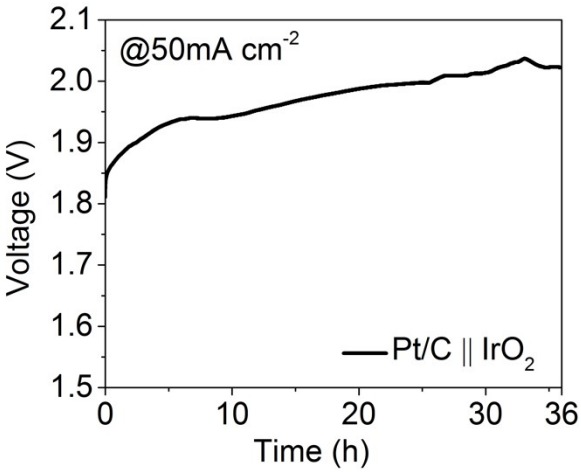

Figure S12. The water splitting durability test of Pt/C || IrO_2 at 50 mA cm^{-2}.

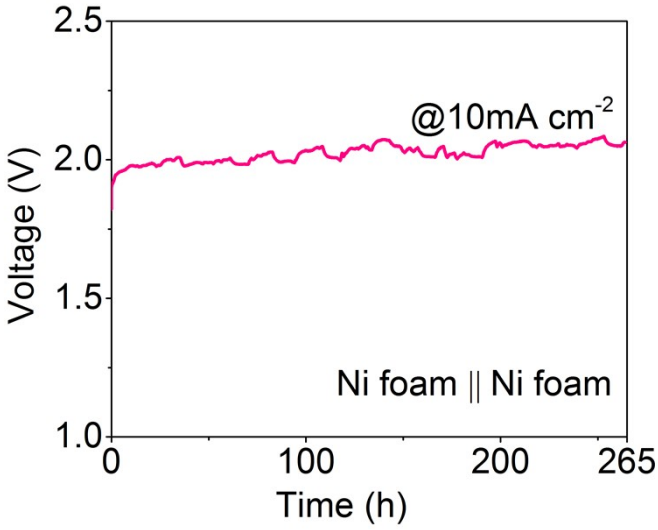

Figure S13. The water splitting durability test of Ni foam || Ni foam at 10 mA cm^{-2}.

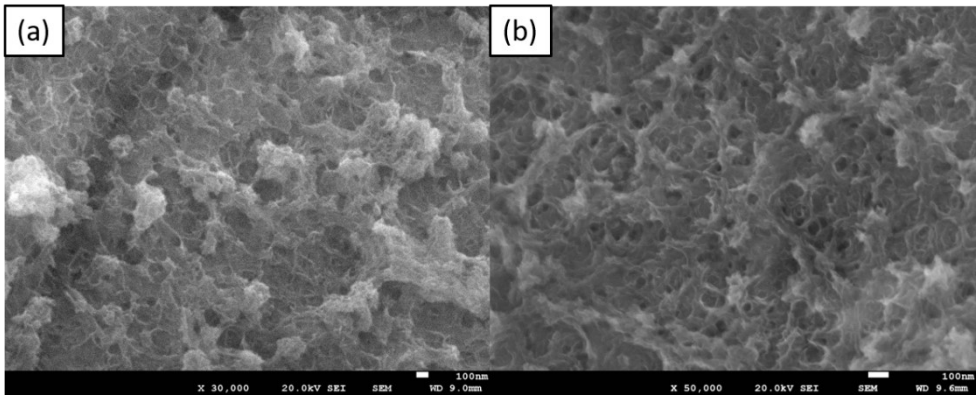

Figure S14. SEM images of RuFe@NF after HER.

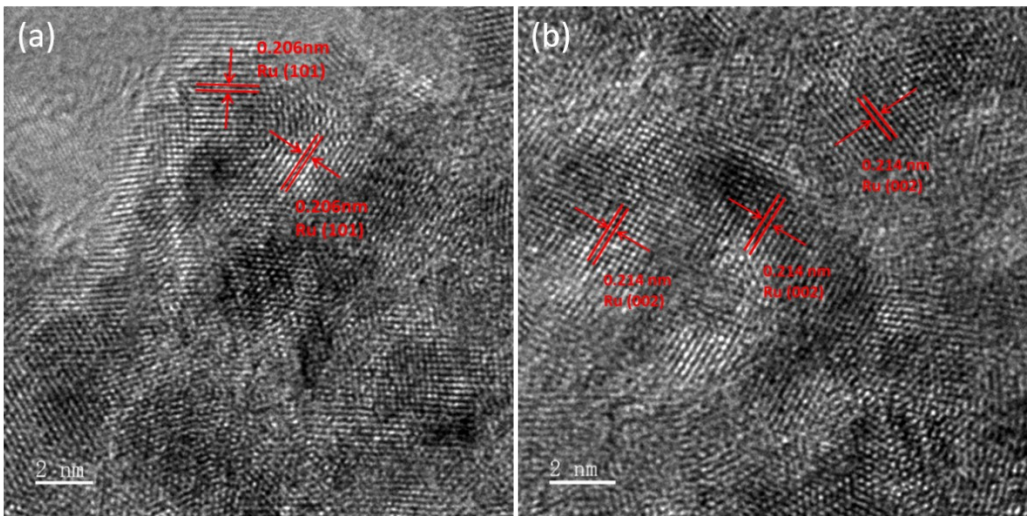

Figure S15. HR-TEM images of RuFe@NF after HER.

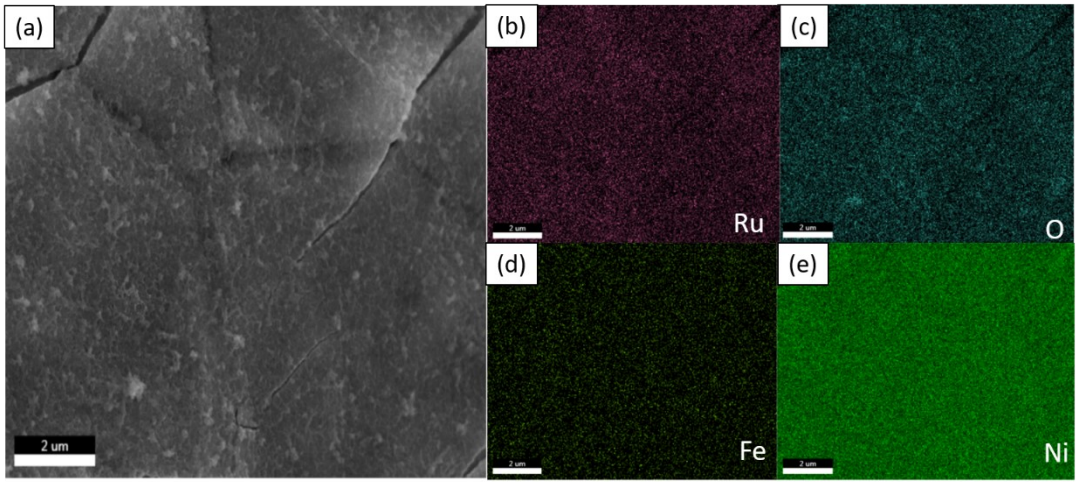

Figure S16. SEM and corresponding element mapping images of RuFe@NF after HER.

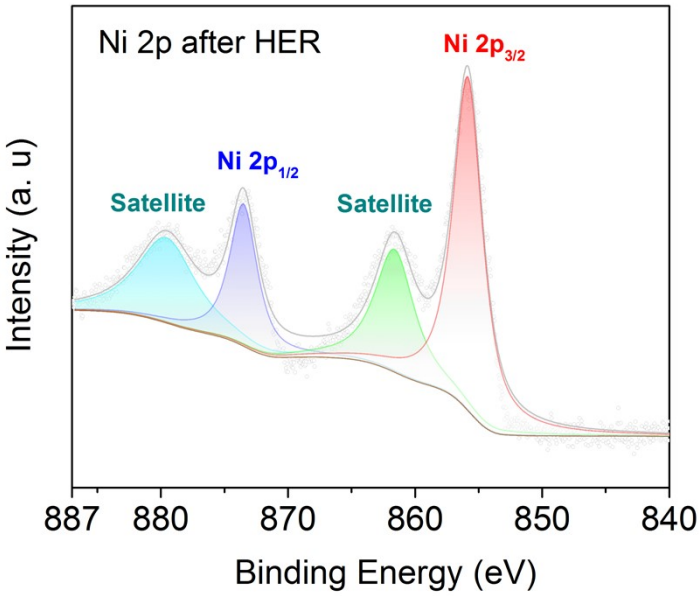

Figure S17. High resolution XPS spectra of Ni 2p of RuFe@NF after HER.

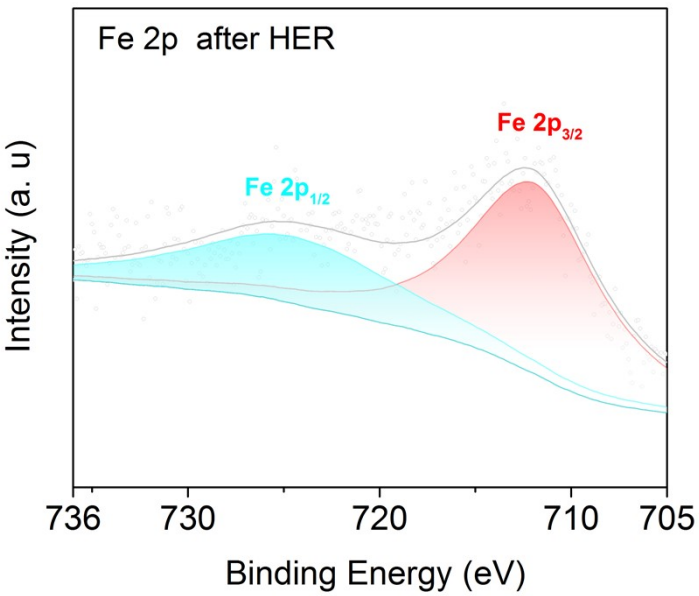

Figure S18. High resolution XPS spectra of Fe 2p of RuFe@NF after HER.

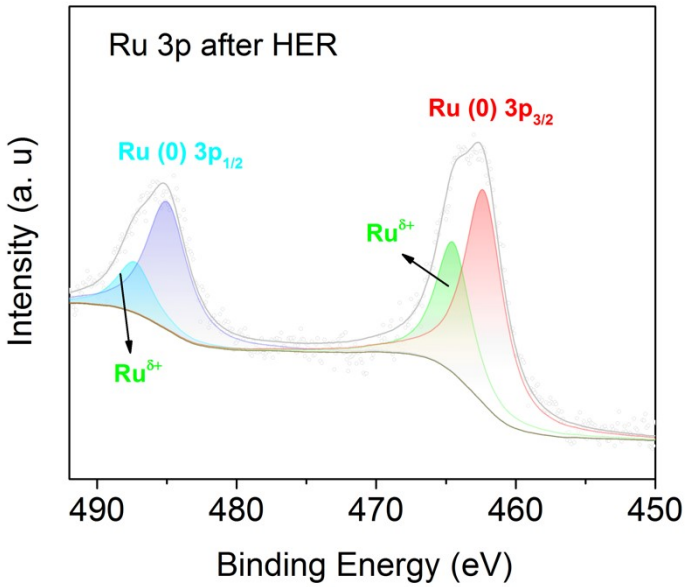

Figure S19. High resolution XPS spectra of Ru 3p of RuFe@NF after HER. The Ru^{n+} appears presumably owing to surface oxidation by the exposure in the air.

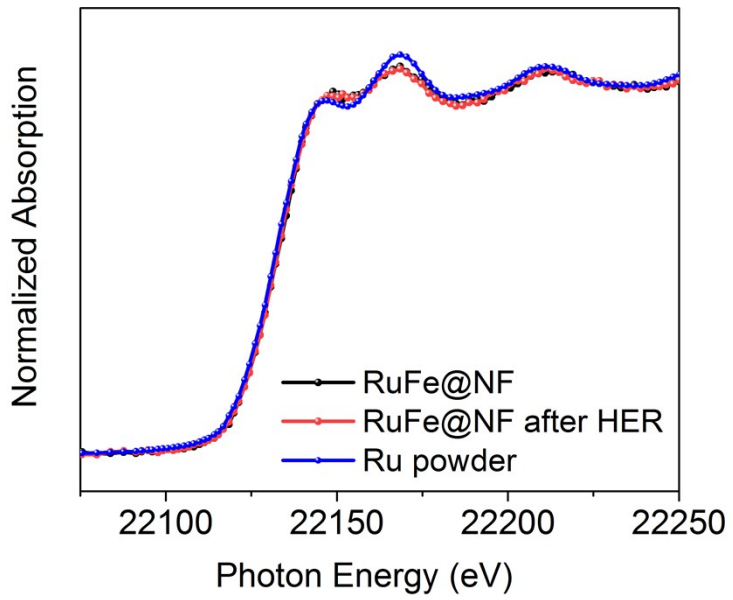

Figure S20. Ru K-edge XANES spectra of the RuFe@NF, RuFe@NF after HER and Ru powder samples.

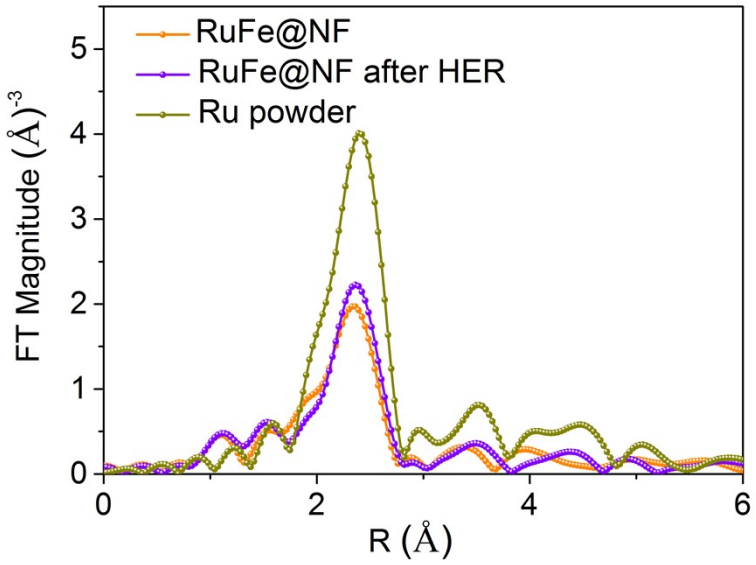

Figure S21. The FT-EXAFS of Ru K-edge spectra of the RuFe@NF, RuFe@NF after HER and Ru powder samples.

Figure S22. The photograph of initial OER at three electrode system.

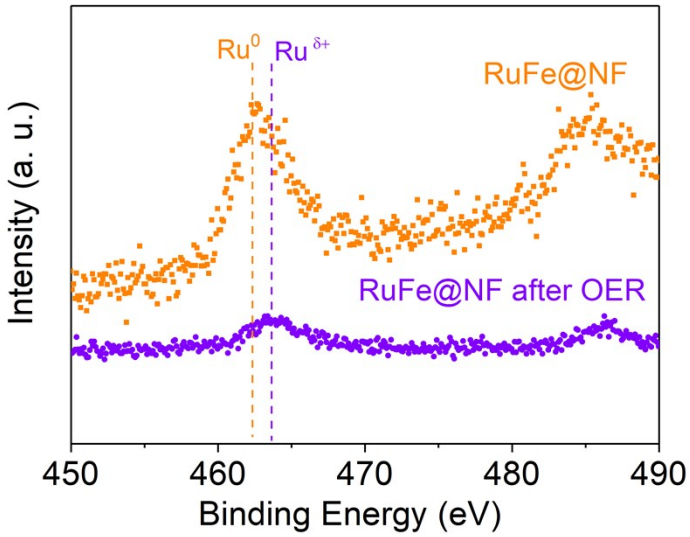

Figure S23. High resolution XPS spectra of Ru 3p of RuFe@NF before and after OER.

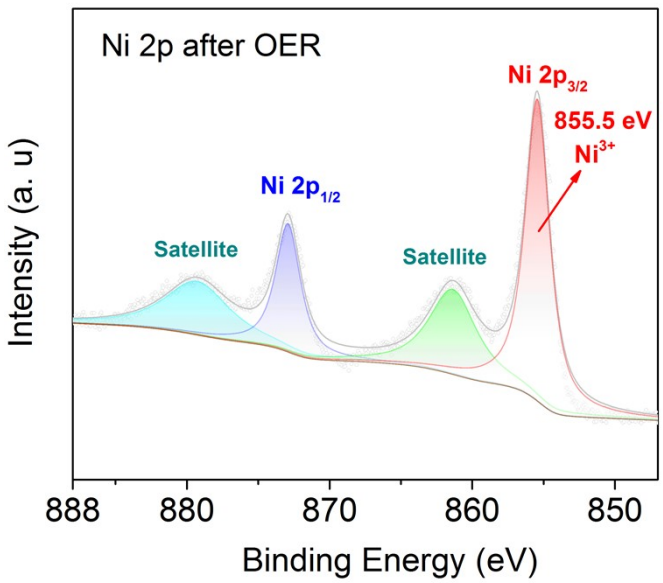

Figure S24. High resolution XPS spectra of Ni 2p of RuFe@NF after OER.

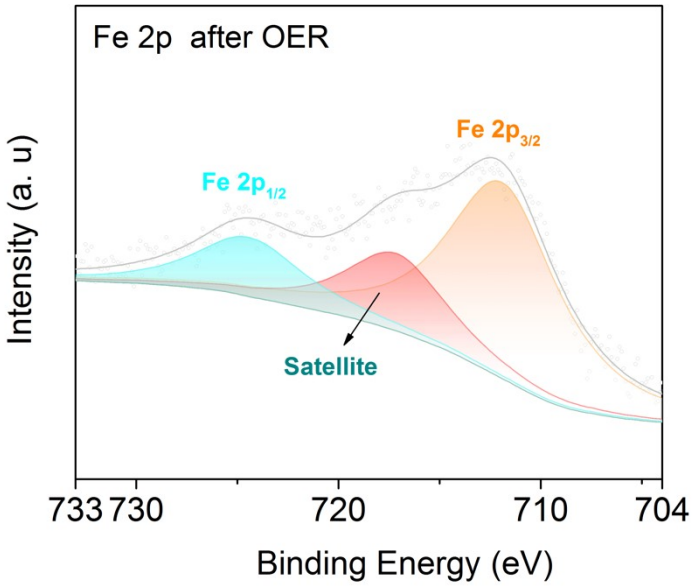

Figure S25. High resolution XPS spectra of Fe 2p of RuFe@NF after OER.

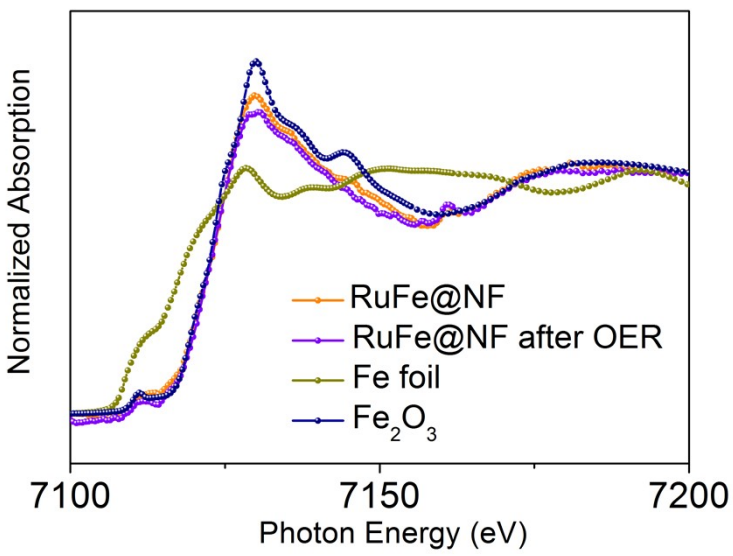

Figure S26. Fe K-edge XANES spectra of the RuFe@NF, RuFe@NF after OER, Fe foil and Fe_2O_3 samples.

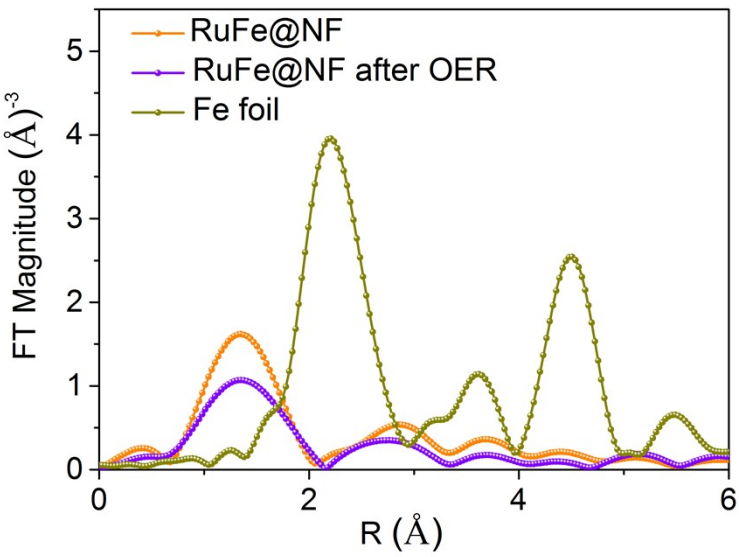

Figure S27. The Fourier transforms and fitting in R space of Fe K-edge spectra for the RuFe@NF, RuFe@NF after OER and Fe foil samples.

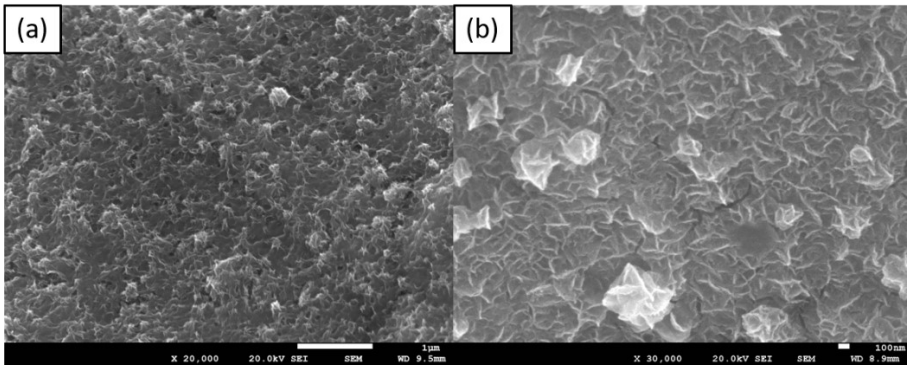

Figure S28. SEM images of RuFe@NF after OER.

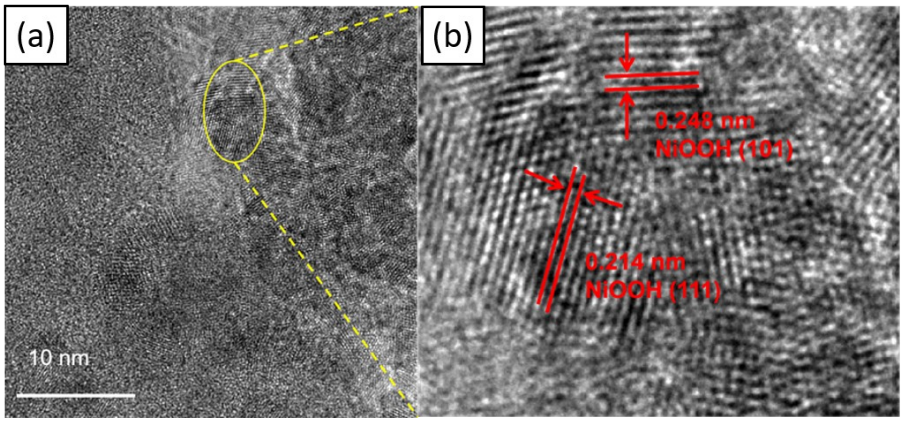

Figure S29. TEM images of RuFe@NF after OER.

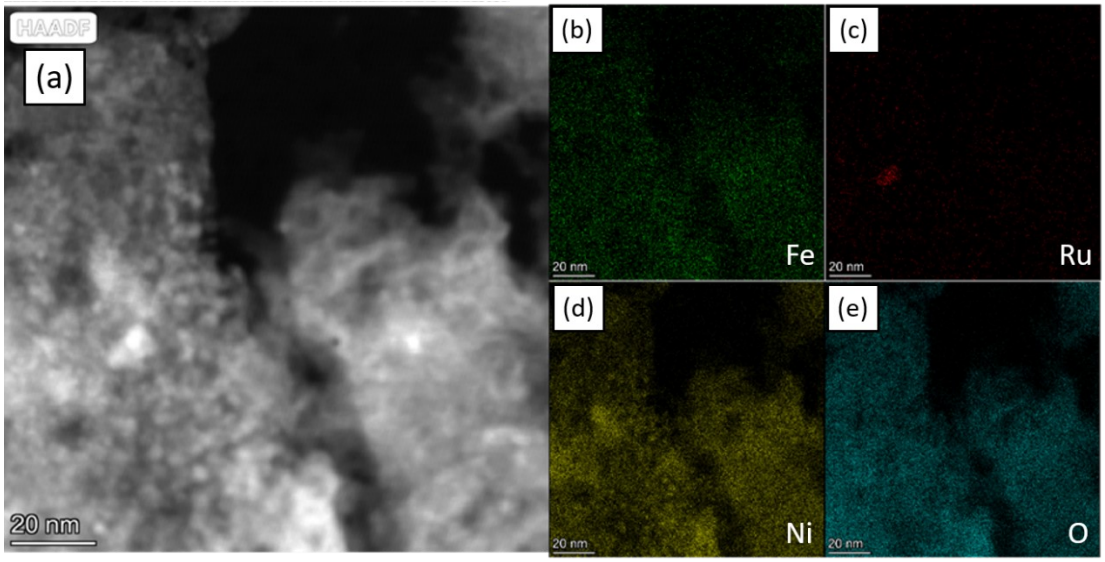

Figure S30. The HAADF-STEM and corresponding element mapping images of RuFe@NF after OER.

Table S1. The water splitting activity of RuFe@NF and other bifunctional OER/HER catalysts reported thus far in alkaline electrolyte.

Electrocatalysts	Support	Electrolyte	η(V) at 10 mA cm^{-2}	References
RuFe@NF	Ni foam	1 M KOH	1.54	*This work*
Co@N-CS/N-HCP@CC	Carbon cloth	1 M KOH	1.545	*Adv. Energy Mater. 2019, 9, 1803918*
SCNF-NR		1 M KOH	1.68	*Adv. Energy Mater. 2017, 7, 1602122*
Ni_5P_4 films	Ni foil	(pH=14)	1.7	*Angew. Chem. Int. Ed. 2015, 54, 12361-12365*
Hierarchical $NiCo_2O_4$	Ni foam	1 M NaOH	1.65	*Angew. Chem. Int. Ed. 2016, 55, 6290-6294*
WN-Ni@N,P-CNT-800		1 M KOH	1.57	*Appl. Catal. B: Environ. 2021, 298, 120511*
Rh SAC−CuO NAs	Copper foam	1 M KOH	1.51	*Nano Lett. 2020, 20, 5482-5489*
NF/T(Ni_3S_2/MnS-O)	Ni foam	1 M KOH	1.54	*Appl. Catal., B 2019, 257, 117899.*
Ni_3S_2/NF	Ni foam	1 M KOH	1.59	*J. Energy Chem. 26 (2017) 1217–1222*
FNHNS/NF	Ni foam	1 M KOH	1.55	*Small 2017, 13, 1602637*
Ir_1@Co/NC		1 M KOH	1.603	*Angew. Chem. Int. Ed. 2019, 58, 11868-11873*
$CoS_{0.58}P_{0.42}$		1 M KOH	1.59	*ACS Nano 2017, 11, 11031-11040*
Ru_2Ni_2SNs/C		1 M KOH	1.68	*Nano Energy 2018, 47, 1–7*
Pt-CoS_2/CC	Carbon cloth	1 M KOH	1.55	*Adv. Energy Mater. 2018, 8, 1800935*
NiFe-MOF-5		1 M KOH	1.57	*Inorg. Chem. Front., 2021, 8, 2889-2899*
CoP NFs	Ni foam	1 M KOH	1.65	*ACS Catal. 2020, 10, 412-419*
Co@Ir/NC-10%		1 M KOH	1.7	*ACS Sustainable Chem. Eng. 2018, 6, 5105-5114*
$Fe_{11\%}$-NiO/NF	Ni foam	1 M KOH	1.579	*J. Catal. 2018, 358, 243-252*
$Fe_{7.4\%}$-NiSe		1 M KOH	1.585	*J. Mater. Chem. A, 2019, 7, 2233–2241*

Hierarchical $NiCo_2S_4$	**Ni foam**	**1 M KOH**	**1.63**	*Adv. Funct. Mater. 2016, 26, 4661-4672*
$RuTe_2$-400		**1 M KOH**	**1.57**	*Appl. Catal. B: Environ. 2020, 278,119281*
a-CoSe film	**Ti mesh**	**1 M KOH**	**1.65**	*Chem. Commun., 2015, 51, 16683-16686*
Ni_2P NPs	**Ni foam**	**1 M KOH**	**1.63**	*J. Mater. Chem. A, 2016, 4, 5639-5646*
Co_3O_4 -MTA	**Ni foam**	**1 M KOH**	**1.63**	*Angew. Chem. Int. Ed. 2017, 56, 1324-1328*
$Fe_{0.29}Co_{0.71}P$/NF	**Ni foam**	**1 M KOH**	**1.64**	*Nano Energy 2020, 67, 104174*

Table S2. The water splitting stability of RuFe@NF and other bifunctional OER/HER catalysts reported thus far in alkaline electrolyte.

Electrocatalysts	Support	Electrolyte	Durability(h)	References
RuFe@NF	**Ni foam**	**1 M KOH**	**700**	*This work*
Rh SAC−CuO NAs	**Copper foam**	**1 M KOH**	**25**	*Nano Lett. 2020, 20, 5482-5489*
Co@N-CS/N-HCP@CC	**Carbon cloth**	**1 M KOH**	**24**	*Adv. Energy Mater. 2019, 9, 1803918*
SCNF-NR		**1 M KOH**	**30**	*Adv. Energy Mater. 2017, 7, 1602122*
Ni_5P_4 films	**Ni foil.**	**(pH=14)**	**20**	*Angew. Chem. Int. Ed. 2015, 54, 12361–12365*
Hierarchical $NiCo_2O_4$	**Ni foam**	**1M NaOH**	**15**	*Angew. Chem. Int. Ed. 2016, 55, 6290-6294*
NiVRu-LDH	**Ni foam**	**1 M KOH**	**300**	*Nat. Commun. 2019, 10, 3899*
Ru-MoS_2-Mo_2C/TiN	**Carbon cloth**	**1 M KOH**	**120**	*Nano Energy, 2021, 88, 106277*
Ni-Mo-P		**1 M KOH**	**40**	*Appl. Catal. B: Environ. 2021, 298, 120494*
WN-Ni@N,P-CNT-800		**1 M KOH**	**10**	*Appl. Catal. B: Environ.2021, 298, 120511*
$Fe_{0.29}Co_{0.71}P$/NF	**Ni foam**	**1 M KOH**	**110**	*Nano Energy 2020, 67, 104174*
NF/T(Ni_3S_2/MnS-O)	**Ni foam**	**1 M KOH**	**50**	*Appl. Catal., B 2019, 257, 117899.*
Ni_3S_2/NF	**Ni foam**	**1 M KOH**	**20**	*J. Energy Chem. 2017, 26, 1217-1222*
Ir_1@Co/NC		**1 M KOH**	**5**	*Angew. Chem. Int. Ed. 2019, 58, 11868-11873*
$CoS_{0.58}P_{0.42}$		**1 M KOH**	**10**	*ACS Nano 2017, 11, 11031-11040*
Ru_2Ni_2SNs/C		**1 M KOH**	**105**	*Nano Energy 2018, 47, 1-7*
Pt-CoS_2/CC	**Carbon cloth**	**1 M KOH**	**20**	*Adv. Energy Mater. 2018, 8, 1800935*
NiFe-MOF-5		**1 M KOH**	**24**	*Inorg. Chem. Front., 2021, 8, 2889-2899*
CoP NFs	**Ni foam**	**1 M KOH**	**30**	*ACS Catal. 2020, 10, 412-419*
Ru-NiCoP/NF	**Ni foam**	**1 M KOH**	**50**	*Appl. Catal. B: Environ.2020,*

				279, 119396
$Fe_{11\%}$-NiO/NF	**Ni foam**	**1 M KOH**	**20**	*Journal of Catalysis 358 (2018) 243–252*
$Fe_{7.4\%}$-NiSe		**1 M KOH**	**27**	*J. Mater. Chem. A, 2019, 7, 2233-2241*
Hierarchical $NiCo_2S_4$	**Ni foam**	**1 M KOH**	**50**	*Adv. Funct. Mater. 2016, 26, 4661-4672*
P-NiFe	**Ni foam**	**1 M KOH**	**100**	*Chem. Sci., 2018, 9, 1375-1384*
$RuTe_2$-400		**1 M KOH**	**20**	*Appl. Catal. B: Environ.2020, 278, 119281*
a-CoSe film	**Ti mesh**	**1 M KOH**	**26**	*Chem. Commun., 2015, 51, 16683-16686.*
Ni_2P NPs	**Ni foam**	**1 M KOH**	**10**	*J. Mater. Chem. A, 2016, 4, 5639-5646*
Co_3O_4 -MTA	**Ni foam**	**1 M KOH**	**12**	*Angew. Chem. Int. Ed. 2017, 56, 1324-1328*

Table S3. The element content of RuFe@NF before and after HER/OER by XPS.

Content	C 1s	Ru 3p	O 1s	Fe 2p	Ni 2p
RuFe@NF	42.98	3.24	39.00	4.03	10.75
RuFe@NF after HER	39.58	5.97	47.18	3.38	3.89
RuFe@NF after OER	31.40	0.71	51.49	6.18	10.22